Journal of Sound and Vibration (1998) **209**(2), 223–249

FINITE ELEMENT ANALYSIS OF A THREE-DIMENSIONAL UNDERWATER CABLE WITH TIME-DEPENDENT LENGTH

P.-H. WANG

Department of Civil Engineering, Chung Yuan Christian University, Chung-Li, Taiwan 32023, *Republic of China*

R.-F. FUNG

Department of Mechanical Engineering, Chung Yuan Christian University, Chung-Li, Taiwan 32023, *Republic of China*

AND

M.-J. LEE

Department of Civil Engineering, Chung Yuan Christian University, Chung-Li, Taiwan 32023, *Republic of China*

(*Received* 30 *September* 1996, *and in final form* 10 *April* 1997)

Three-dimensional underwater vibrations of a geometrically non-linear cable with a weight at the lower end are investigated. The length of the cable is time-dependent. A set of non-linear, time-varying differential equations describing this system is derived by Hamilton's principle and the variable-domain finite element method. The results of numerical simulation are presented for constant-speed and sinusoidal axial motions of the cable. The vibration responses of three initial conditions are shown. The effects of initial displacements, initial tensions due to gravity and the hydrodynamic forces on the non-linear longitudinal and transverse amplitudes are presented. Finally, some conclusions are drawn.

1. INTRODUCTION

Submerged cables are used extensively in oceanographic research, hydrographic surveying, salvage, telecommunications, fishing, offshore technology and towing. These areas in engineering applications require accurate analysis to predict their static and dynamic behavior. Various approaches have been devoted to the analysis of underwater cable systems. Analyses of the three-dimensional (3-D) motion of a towed cable system can be found in an article by Sanders [1]. The finite difference method was employed but the inertial forces were ignored. Delmer *et al*. [2] used the finite element method to handle cables with time-varying length. Ablow *et al*. [3] used the finite difference method in the local cable coordinate formulation. Milinazzo *et al*. [4] employed a second-order finite difference approximation for the governing equations of the 3-D motion of a towed cable. Delmer *et al*. [5] studied the 3-D geometric behavior of cable-towed acoustic array systems by using the lumped element method and the stiff integration. Hann [6] analyzed planar oscillation of hoisting cables for submersibles. Hover *et al*. [7] extended a matrix method for mooring systems to address the dynamic responses of towed underwater systems.

0022–460X/98/020223 + 27 $25.00/0/sv971227

Banerjee and Do [8] modelled an underwater cable as a chain of rigid rods which are connected to one another by two-degree-of-freedom hinges in conjunction with soft rotational springs. Khan and Ansar [9] derived equations of motion for a multi-component mooring cable by using Lagrange's modified equation. However, these studies consider a cable system of fixed length with no axial motion.

Recently, vibration of axially moving materials has received a great deal of attention in literature. A comprehensive review of the extensive researches in all types of axially moving material problems has been presented by Wickert and Mote [10]. In most of these studies, the equations of motion are described on a fixed spatial domain. Vibration problems of materials whose effective lengths vary with time have been the subject of recent interest. Tabarrok *et al*. [11] studied the problem of a cantilever beam whose length varies with time. They used Newton's second law to derive the equations of motion. Approximate solutions were based on the Galerkin method associated with time-dependent basis functions. This approach method was also used by Wang and Wei [12] to analyze vibrations for a moving flexible robot arm; by Yuh and Young [13] to study the dynamic modelling of an axially moving beam in rotation; and by Fung and Cheng [14] to investigate the free vibration of a non-linear coupled string/slider system with a moving boundary.

A related problem involving free vibration induced by initial displacements for a string was presented in a series of papers by Kotera and co-workers [15–19]. In these studies, the string length is time-dependent, a linear damping is considered and a weight is attached at one end of the string. Stylianou and Tabarrok [20] studied an axially moving beam and used the finite element method to obtain the transient amplitudes. Al-Bedoor and Khulief [21] studied the vibrations of an elastic beam with prismatic and revolute joints by using the Lagrangian approach in conjunction with the assumed modes technique. Terumichi *et al*. [22] studied the non-stationary vibrations of a string with time-varying length, and a mass-spring system attached at the lower end.

In studying the vibration problems of strings with time-dependent lengths, the methods of solving these problems inevitably differ from the classical methods of treating the fixed domain problems. For instance, the concept of natural modes and frequencies becomes meaningless because the natural frequencies become time-dependent as the length of the string varies and the independence of natural modes of oscillation is lost. Traditionally, the finite element formulations are normally carried out by using the fixed-size element length. In order to analyze the problems with time-dependent domains, the technique of finite element analysis [20] is utilized in this paper. While the number of elements remains fixed, the size of the elements changes with time. To this end, a variable-size finite element is formed with the size having a prescribed function of time.

The objective in this study, is to investigate the dynamics of an underwater, drawn cable with an attached mass. The analysis includes gravitational and hydrodynamic effects as well as the drag and inertia effects of water on the cable. The investigation begins with the derivation of a continuum model describing the cable spatial response. A set of non-linear equations governing the motion of a cable with time-varying length is derived by Hamilton's principle. A variable-domain finite element method is used to discretize the non-linear equations, and the Runge–Kutta method is used to integrate the discretized equation. The numerical simulations for various parameters are conducted.

2. SYSTEM DESCRIPTION

As illustrated in Figure 1, a co-ordinate system x, y, z with unit vectors $\mathbf{i}, \mathbf{j}, \mathbf{k}$ is used to describe the cable configuration. An axially moving cable is modelled as a 1-D,

homogeneous elastic continuum which obeys the linear stress–strain law. The cable is wound on a drum at the top end and is attached with a mass m at the lower end. Three different configurations are distinguished: (i) the characteristics of the cable in the natural configuration (zero stress and strain field) are ρ^0, mass per unit length, A, area of the normal section, E, elastic material modulus; (ii) in initially stressed configuration P, the length at time t is $l(t)$, transport velocity of cable particles is $\dot{x}$ and acceleration is $\ddot{x}$; (iii) the deformed configuration P^v is occupied by the cable during the motion under static and dynamic loads.

2.1. KINETIC AND STRAIN ENERGIES

The position vector of a material particle in configuration P on the axially moving cable is

$$\mathbf{r} = x(t)\mathbf{i}. \tag{1}$$

Since the cable has axial motion, the position x is a function of time. By assuming P to be the reference configuration for the cable motion, the dynamic displacement

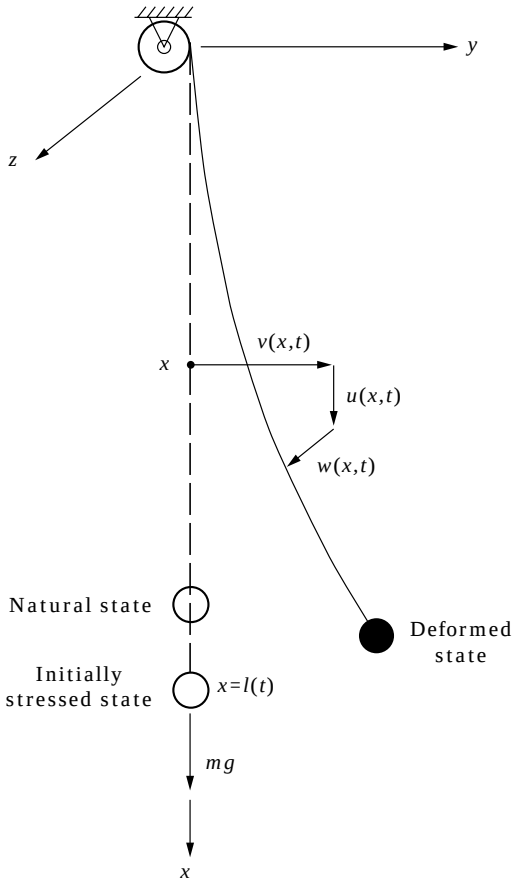

Figure 1. Cable with time-varying length.

vector is given by

$$\mathbf{u}(x, t) = u(x, t)\mathbf{i} + v(x, t)\mathbf{j} + w(x, t)\mathbf{k}, \tag{2}$$

where u, v, and w are displacements in three directions, respectively. Then, the position vector of a material particle on the cable in configuration P^v is expressed as

$$\mathbf{r}^v = \mathbf{r} + \mathbf{u} = [x(t) + u(x, t)]\mathbf{i} + v(x, t)\mathbf{j} + w(x, t)\mathbf{k}. \tag{3}$$

The Lagrangian strain in P^v is defined as

$$\varepsilon^v = \tfrac{1}{2}\left(\frac{\partial \mathbf{r}^v}{\partial x^0} \cdot \frac{\partial \mathbf{r}^v}{\partial x^0} - 1\right), \tag{4}$$

in which x^0 denotes the position of the material particle on the cable in the natural configuration.

Since the cable is hung under not only the weight of the attached mass but also its own weight, the initial tension H can be expressed as

$$H(x) = mg + \rho g(l - x), \tag{5}$$

where ρ is the mass per unit length in configuration P and g is the gravitational acceleration. The conservation of mass states that

$$\rho = \rho^0 \frac{\mathrm{d}x^0}{\mathrm{d}x} = \frac{\rho^0}{1 + \varepsilon_0}, \tag{6}$$

where

$$\varepsilon_0 = \frac{H}{EA}$$

is the initial strain due to the initial tension and EA is the axial rigidity.

The initial Lagrangian strain is defined as

$$\varepsilon^i = \tfrac{1}{2}\left[\left(\frac{\mathrm{d}x}{\mathrm{d}x^0}\right)^2 - 1\right] = \varepsilon + \tfrac{1}{2}\varepsilon^2, \tag{7}$$

where ε is the additional Lagrangian strain which refers to the initially stressed configuration P

$$\varepsilon = \frac{\partial u}{\partial x} + \tfrac{1}{2}\frac{\partial u}{\partial x}\frac{\partial u}{\partial x} = u_x + \tfrac{1}{2}(u_x^2 + v_x^2 + w_x^2), \tag{8}$$

and the subscript x denotes the partial derivatives with respect to the spatial variable x.

The incremental strain energy [23] of the whole cable from the static equilibrium can be expressed as the sum of the potential energy due to the initial tension, and the potential energy due to the dynamic stress and strain. Thus, the strain energy is

$$\begin{aligned} U &= (1 + \varepsilon_0)\int_0^{l(t)} [H\varepsilon + \tfrac{1}{2}k\varepsilon^2]\,\mathrm{d}x \\ &= (1 + \varepsilon_0)\int_0^{l(t)} \{H[u_x + \tfrac{1}{2}(u_x^2 + v_x^2 + w_x^2)] \\ &\quad + \tfrac{1}{2}k[u_x^2 + u_x(u_x^2 + v_x^2 + w_x^2) + \tfrac{1}{4}(u_x^2 + v_x^2 + w_x^2)^2]\}\,\mathrm{d}x, \end{aligned} \tag{9}$$

where

$$k = EA\left(\frac{\mathrm{d}x}{\mathrm{d}x^0}\right)^3, \frac{\mathrm{d}x}{\mathrm{d}x^0} = 1 + \varepsilon_0. \tag{10}$$

It is seen that coupling between three displacements u, v and w is shown in the strain energy function.

The velocity vector of a material particle can be obtained by differentiating equation (3) with respect to time,

$$\mathbf{v}_c = \frac{\mathrm{d}\mathbf{r}^p}{\mathrm{d}t} = (\dot{x} + u_t + \dot{x}u_x)\mathbf{i} + (v_t + \dot{x}v_x)\mathbf{j} + (w_t + \dot{x}w_x)\mathbf{k}, \tag{11}$$

where the subscript c denotes the cable and subscripts t and x denote partial derivatives with respect to temporal variable t and spatial variable x, respectively. The dot means $\mathrm{d}/\mathrm{d}t$, $\dot{x}$ is the axial velocity of the cable. Then, the acceleration vector of a cable particle is

$$\mathbf{a}_c = \frac{\mathrm{d}\mathbf{v}_c}{\mathrm{d}t} = (\ddot{x} + u_{tt} + 2\dot{x}u_{xt} + \dot{x}^2u_{xx})\mathbf{i} + (v_{tt} + 2\dot{x}v_{xt} + \dot{x}^2v_{xx})\mathbf{j} + (w_{tt} + 2\dot{x}w_{xt} + \dot{x}^2w_{xx})\mathbf{k}, \tag{12}$$

in which $(\,)_{tt}$, $2\dot{x}(\,)_{xt}$ and $\dot{x}^2(\,)_{xx}$ are the local, Coriolis and centripetal components of acceleration, respectively [24]. The acceleration vector (12) will be used in the hydrodynamic force. The velocity vector obtained in equation (11) is used to obtain the kinetic energy of the cable as

$$\begin{aligned} T &= \tfrac{1}{2}\int_0^{l(t)} \rho\mathbf{v}_c \cdot \mathbf{v}_c \,\mathrm{d}x \\ &= \tfrac{1}{2}\int_0^{l(t)} \rho(\dot{x}^2 + 2\dot{x}u_t + 2\dot{x}^2u_x + u_t^2 + \dot{x}^2u_x^2 + 2\dot{x}u_tu_x \\ &\quad + v_t^2 + \dot{x}^2v_x^2 + 2\dot{x}v_tv_x + w_t^2 + \dot{x}^2w_x^2 + 2\dot{x}w_tw_x)\,\mathrm{d}x. \end{aligned} \tag{13}$$

2.2. VIRTUAL WORK

The virtual work is done by the external forces which include the fluid force $\mathbf{f}$ acting on the cable and the interaction force $\mathbf{R}$ between the cable and the attached mass. The virtual work can be expressed as

$$\delta W = -\mathbf{R} \cdot \delta\mathbf{u}(l, t) + \int_0^{l(t)} \mathbf{f} \cdot \delta\mathbf{u}\,\mathrm{d}x, \tag{14}$$

where $\delta\mathbf{u}$ denotes virtual displacement. In the following two sections, the fluid force $\mathbf{f}$ and the interaction force $\mathbf{R}$ are to be described.

2.2.1. *Virtual work due to hydrodynamic force*

The dynamic behavior of a cable submerged in water is affected primarily by the non-linear and non-conservative fluid force. The fluid force consists of: (i) inertial force which is due to the fluid acceleration relative to the cable; (ii) drag force which is associated

with the relative velocity, acts as the damping force [25] and has a great effect on the slow drift oscillation; (iii) buoyancy force which is small enough to be negligible.

It is assumed in this paper that the fluid is incompressible, the diameter of the cable is d and the fluid mass density is ρ_f. Using the results of Webster [25], the fluid force per unit length of a cylindrical cable may be expressed as:

$$\begin{aligned}\mathbf{f} &= \mathbf{f}_{AM} + \mathbf{f}_{DN} + \mathbf{f}_{DT} \\ &= C_M \rho_f (\pi/4)\, \mathrm{d}^2\mathbf{a}_N + C_N \rho_f (d/2)|\mathbf{v}_N|\mathbf{v}_N + C_T \rho_f (d/2)|\mathbf{v}_T|\mathbf{v}_T,\end{aligned} \tag{15}$$

where $\mathbf{f}_{AM}$ is the inertia force due to the added mass, $\mathbf{f}_{DN}$ is the normal drag force, $\mathbf{f}_{DT}$ is the tangential drag force, $\mathbf{v}_N$ and $\mathbf{v}_T$ are the normal and tangential components of the fluid velocity relative to the cable, and $\mathbf{a}_N$ is the normal component of the fluid acceleration relative to the cable. The tangential (normal) drag force is proportional to the square of tangent (normal) fluid speed relative to the cable. C_M is the coefficient of the added mass, C_N and C_T are respectively the normal and tangential drag coefficients which are dependent on Reynold's number of the fluid speed relative to the cable segment. They are usually determined experimentally and the reported values may vary slightly. Webster [25] recorded them as

$$C_M = \quad 1{\cdot}0, \tag{16a}$$

$$C_N = \begin{cases} 0{\cdot}0, & \text{for } R_{eN} \leqslant 0{\cdot}1 \\ 0{\cdot}45 + 5{\cdot}93/(R_{eN})^{0{\cdot}33}, & \text{for } 0{\cdot}1 \leqslant R_{eN} \leqslant 400 \\ 1{\cdot}27, & \text{for } 400 \leqslant R_{eN} \leqslant 10^5 \\ 0{\cdot}3, & \text{for } 10^5 \leqslant R_{eN} \end{cases} \tag{16b}$$

$$C_T = \begin{cases} 1{\cdot}88/(R_{eT})^{0{\cdot}74}, & \text{for } 0{\cdot}1 \leqslant R_{eT} \leqslant 100{\cdot}55 \\ 0{\cdot}062, & \text{for } 100{\cdot}55 \leqslant R_{eT} \end{cases} \tag{16c}$$

where the Reynold's numbers R_{eN} and R_{eT} are defined as

$$R_{eN} = \rho\ \mathrm{d}|\mathbf{v}_N|/\mu, \qquad R_{eT} = \rho\ \mathrm{d}|\mathbf{v}_T|/\mu, \tag{17}$$

and μ is the viscosity of the fluid.

In order to calculate the hydrodynamic force (15), the fluid normal acceleration a_N, normal velocity $\mathbf{v}_N$ and tangent velocity $\mathbf{v}_T$ must be determined first for each segment in the finite element method.

2.2.2. *Virtual work due to the attached mass*

The interaction force between the cable and the attached mass is

$$\mathbf{R} = m \frac{\mathrm{d}^2}{\mathrm{d}t^2} \mathbf{r}|_{x = l(t)} = m\mathbf{a}_c|_{x = l(t)}. \tag{18}$$

From equation (12), the magnitude of the component of $\mathbf{R}$ is

$$R_u = \mathbf{R} \cdot \mathbf{i} = m(\ddot{x} + u_{tt} + 2\dot{x}u_{xt} + \dot{x}^2 u_{xx})_{x = l(t)}, \tag{19a}$$

$$R_v = \mathbf{R} \cdot \mathbf{j} = m(v_{tt} + 2\dot{x}v_{xt} + \dot{x}^2 v_{xx})_{x = l(t)}, \tag{19b}$$

$$R_w = \mathbf{R} \cdot \mathbf{k} = m(w_{tt} + 2\dot{x}w_{xt} + \dot{x}^2 w_{xx})_{x = l(t)}. \tag{19c}$$

3. FINITE ELEMENT DISCRETIZATION

In this paper, a variable-domain element [20] is used and the number of elements remains fixed. In the finite element method, the continuous displacements may be approximated in terms of the discretized nodal displacements. The element model presented here consists of two nodes and each node has the axial deflection u, and the lateral deflections v and w. Each of these continuous deflections of a typical point within the jth element can be related to the discretized nodal displacement vectors $\mathbf{q}_{uj}$, $\mathbf{q}_{vj}$ and $\mathbf{q}_{wj}$ as well as the shape function matrices $\mathbf{N}_j$ as

$$\begin{aligned} u(x,t) &= \mathbf{N}_j(x, l(t))\mathbf{q}_{uj}(t), \\ v(x,t) &= \mathbf{N}_j(x, l(t))\mathbf{q}_{vj}(t), \qquad x_j \leqslant x \leqslant x_{j+1}, \qquad j = 1, 2, \ldots, n \\ w(x,t) &= \mathbf{N}_j(x, l(t))\mathbf{q}_{wj}(t), \end{aligned} \tag{20}$$

where n is the number of finite elements in the discretization of the cable and $\mathbf{q}_{uj}$, $\mathbf{q}_{vj}$ and $\mathbf{q}_{wj}$ are the 2×1 nodal displacement vectors for the deflections u, v and w, respectively. $\mathbf{N}_j$ is the shape function derived from the element displacement field and is given by

$$\mathbf{N}_j = \left[\frac{x_{j+1} - x}{x_{j+1} - x_j}, \frac{x - x_j}{x_{j+1} - x_j}\right] = \frac{n}{l}\left[\frac{j}{n}l - x, x - \frac{j-1}{n}l\right]. \tag{21}$$

It is worth noting that $\mathbf{N}_j$ is a function of x and $l(t)$. Some derivatives of the shape functions are

$$\begin{aligned} \mathbf{N}_{jt} &= \frac{n\dot{l}}{l^2}[x, -x], & \mathbf{N}_{jtt} &= (l\ddot{l} - 2\dot{l}^2)\frac{n}{l^3}[x, -x], \\ \mathbf{N}_{jx} &= \frac{1}{h_j}[-1, 1] = \frac{n}{l}[-1, 1], & \mathbf{N}_{jxt} &= \frac{n\dot{l}}{l^2}[1, -1]. \end{aligned} \tag{22}$$

3.1. KINETIC AND STRAIN ENERGIES

Substituting equations (20) into equations (9) and (13), the element Lagrangian of the cable system can be written in terms of $\mathbf{N}_j$, $\mathbf{q}_{uj}$, $\mathbf{q}_{vj}$ and $\mathbf{q}_{wj}$ and their derivatives. That is

$$L_j = T_j - U_j, \tag{23}$$

where T_j and U_j are detailed in the Appendix.

3.2. VIRTUAL WORK

The virtual work done by the fluid force for the jth element can be expressed as

$$\delta W_j = \int_{x_j}^{x_{j+1}} (f_x \delta u + f_y \delta v + f_y \delta w)\, \mathrm{d}x, \tag{24}$$

where f_x, f_y and f_z are three components of the fluid forces $\mathbf{f}$ shown in equation (17) and $\delta u = \delta\mathbf{q}_{uj}^T\mathbf{N}_j^T$, $\delta v = \delta\mathbf{q}_{vj}^T\mathbf{N}_j^T$ and $\delta w = \delta\mathbf{q}_{wj}^T\mathbf{N}_j^T$ are the virtual displacements. Hence, equation (24) can be rewritten as

$$\begin{aligned} \delta W_j &= \delta\mathbf{q}_{uj}^T \int_{x_j}^{x_{j+1}} \mathbf{N}_j^T f_x \,\mathrm{d}x + \delta\mathbf{q}_{vj}^T \int_{x_j}^{x_{j+1}} \mathbf{N}_j^T f_y \,\mathrm{d}x + \delta\mathbf{q}_{wj}^T \int_{x_j}^{x_{j+1}} \mathbf{N}_j^T f_z \,\mathrm{d}x \\ &= \delta\mathbf{q}_{uj}^T\mathbf{f}_{xj} + \delta\mathbf{q}_{vj}^T\mathbf{f}_{yj} + \delta\mathbf{q}_{wj}^T\mathbf{f}_{zj}, \end{aligned} \tag{25}$$

where $\mathbf{f}_{xj}$, $\mathbf{f}_{yj}$, $\mathbf{f}_{zj}$ are the generalized forces in the x, y and z directions, respectively, and can be expressed as

$$\mathbf{f}_{xj} = \int_{x_j}^{x_{j+1}} \mathbf{N}_j^T f_x \, \mathrm{d}x, \qquad \mathbf{f}_{yj} = \int_{x_j}^{x_{j+1}} \mathbf{N}_j^T f_y \, \mathrm{d}x, \qquad \mathbf{f}_{zj} = \int_{x_j}^{x_{j+1}} \mathbf{N}_j^T f_z \, \mathrm{d}x. \tag{26}$$

The components of the hydrodynamic force (15) are shown in the Appendix.

Substituting equation (20) into equation (18), we obtain the interaction force in terms of $\mathbf{N}_j$, $\mathbf{q}_{uj}$, $\mathbf{q}_{vj}$ and $\mathbf{q}_{wj}$. Finally, the virtual work (14) done by both the fluid force and the interaction force (18) between the cable and the attached mass is

$$\delta W = -\mathbf{R} \cdot \delta \mathbf{u}(l, t) + \sum_{j=1}^{n} \delta W_j. \tag{27}$$

3.3. EQUATIONS OF MOTION

The equations of motion will be obtained by substituting the element Lagrangian (23) and the virtual work (27) into Hamilton's principle:

$$\int_{t_1}^{t_2} \left[\sum_{j=1}^{n} (\delta L_j + \delta W_j) - \mathbf{R} \cdot \delta \mathbf{u}(l, t) \right] \mathrm{d}t = 0, \tag{28}$$

where t_1 and t_2 are two arbitrary times and n is the number of the element. The assembled global finite element equations are

$$\begin{bmatrix} \mathbf{M} & 0 & 0 \\ 0 & \mathbf{M} & 0 \\ 0 & 0 & \mathbf{M} \end{bmatrix} \begin{Bmatrix} \ddot{\mathbf{Q}}_u \\ \ddot{\mathbf{Q}}_v \\ \ddot{\mathbf{Q}}_w \end{Bmatrix} + \begin{bmatrix} \mathbf{C} & 0 & 0 \\ 0 & \mathbf{C} & 0 \\ 0 & 0 & \mathbf{C} \end{bmatrix} \begin{Bmatrix} \dot{\mathbf{Q}}_u \\ \dot{\mathbf{Q}}_v \\ \dot{\mathbf{Q}}_w \end{Bmatrix} + \begin{bmatrix} \mathbf{K}_u & 0 & 0 \\ 0 & \mathbf{K}_v & 0 \\ 0 & 0 & \mathbf{K}_w \end{bmatrix} \begin{Bmatrix} \mathbf{Q}_u \\ \mathbf{Q}_v \\ \mathbf{Q}_w \end{Bmatrix} + \begin{Bmatrix} \mathbf{S}_u^n \\ \mathbf{S}_v^n \\ \mathbf{S}_w^n \end{Bmatrix} = \begin{Bmatrix} \mathbf{F}_u \\ \mathbf{F}_v \\ \mathbf{F}_w \end{Bmatrix}, \tag{29}$$

where the matrices are shown in the Appendix. The above equation is a set of non-linear, second-order differential equations with variable coefficients.

If the motion of the cable is confined to the x–y plane, only the displacement components u and v are considered. The equations of motion of the 2-D system can be obtained from equation (29) by eliminating the displacement component $\mathbf{Q}_w$. For a 1-D model, i.e., only the displacement v is considered, the equations can also easily be deduced.

4. NUMERICAL RESULTS AND DISCUSSION

The non-linear governing equations (29) are the second-order differential equations with variable coefficients. They will be used to investigate the dynamic responses of a cable undergoing various prescribed motions. The solutions of the equations are obtained by the Runge–Kutta method (RK45). Kotera [15–19] published a series of studies on vibrations of a string with time-varying length. However, these studies considered the string with uniform motions only. In this study, we will consider the constant-speed and the sinusoidal axial motions.

4.1. CONSTANT-SPEED AXIAL MOTION

The following function form for $l(t)$ is used to generate the constant-speed axial motion

$$l(t) = l_0 + v_0 t, \tag{30}$$

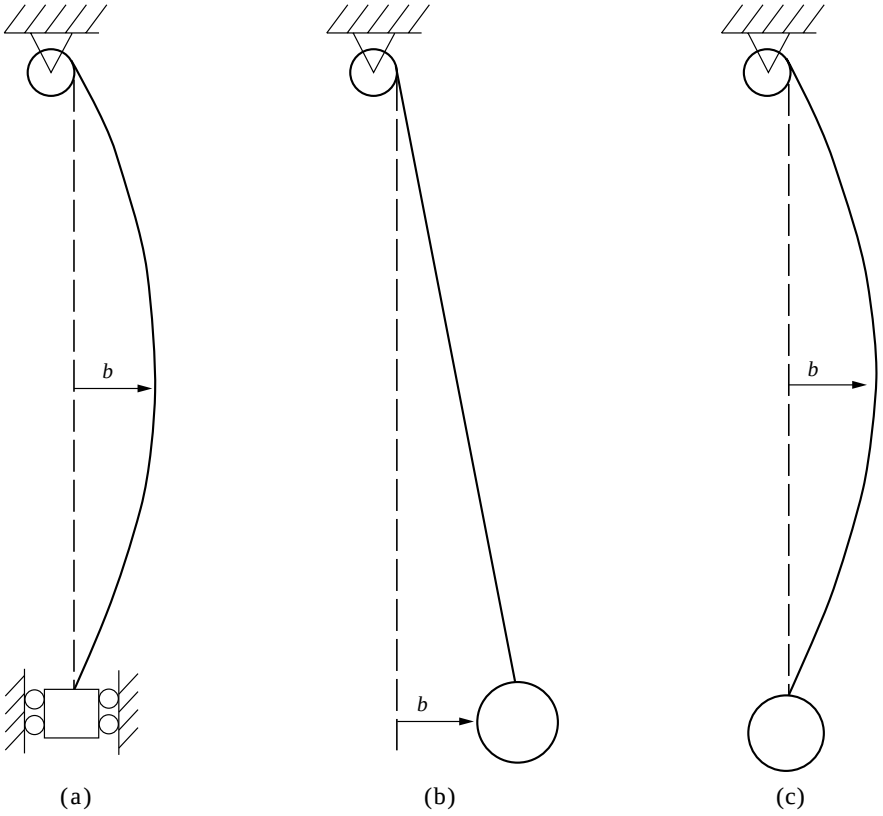

Figure 2. Various initial conditions.

where l_0 and v_0 are the initial length and velocity of the cable, respectively. We will investigate the responses of the cable by specifying different values of the initial length and velocity.

4.2. SINUSOIDAL AXIAL MOTION

This is an ideal case for the velocity and the acceleration being constant. In this section, we consider the axial motion with a variation in velocity, which is taken as

$$\dot{x}(t) = v_0 + v_1 \sin \omega t, \tag{31}$$

where v_0 is the steady-state velocity, v_1 and ω are the amplitude and frequency of the axial perturbing velocity, respectively. Therefore

$$\dot{x}^2(t) = v_0^2 + \tfrac{1}{2}v_1^2 + 2v_0 v_1 \sin \omega t - \tfrac{1}{2}v_1 \cos 2\omega t, \tag{32}$$

$$\ddot{x}(t) = \omega v_1 \cos \omega t. \tag{33}$$

It is noticed that equation (A13) in the Appendix includes $\dot{x}$, $\dot{x}^2$ and $\ddot{x}$. From equations (31)–(33), it is seen that $\sin \omega t$, $\cos \omega t$ and $\cos 2\omega t$ terms are included in the element matrices. Thus, the parametric excitation may occur at both frequencies ω and 2ω of the perturbed velocity.

Three initial conditions of the cable and its attached mass are shown in Figures 2(a)–(c). The numerical results and discussions of these three initial conditions will be exploited in the following sections.

4.3. SIMPLY SUPPORTED CONDITION

Consider the free vibration of a simply supported cable shown in Figure 2(a). An initial displacement is

$$v(x, 0) = b \sin\left(\frac{\pi x}{l_0}\right), \qquad v_t(x, 0) = 0, \tag{34}$$

where b is the initial displacement in the midpoint of the cable. In the 2- and 3-D models, the initial displacement and velocity in the longitudinal direction are given as

$$u(x, 0) = -\frac{\pi}{8}\frac{b^2}{l_0} \sin\left(\frac{2\pi x}{l_0}\right), \qquad u_t(x, 0) = 0, \tag{35}$$

respectively, then the tension in the statically displaced cable is almost constant [26].

In the following numerical examples, the dimensions and properties of the cable are: the initial tension is given in equation (5) and $mg = 10^2 N$, mass per unit length $\rho = 1$ kg/m, rigidity $EA = 10^4 N$ and initial length $l_0 = 0{\cdot}5$ m.

In order to choose an appropriate element number for the finite element analysis, the case for a cable with $b = 0{\cdot}01 l_0$ is first considered. With the above dimensions and properties, the periods associated with the first natural frequencies in the transverse and longitudinal directions are 0·1 and 0·01 s, respectively. The results of transverse vibration of the 1-D model with element numbers $n = 4, 8, 16, 32$ are shown in Figure 3. It is obvious that the response for $n = 16$ is very close to that for $n = 32$. Thus, the convergence is achieved when $n = 16$ is used in all the following numerical examples.

A cable with an initial length $l_0 = 0{\cdot}5$ m, a small initial displacement $b = 0{\cdot}005$ m (Figure 4), and a large initial displacement $b = 0{\cdot}05$ m (Figure 5) is studied for 1- and 2-D non-linear vibrations. Figures 4(a) and (c) show the transverse and longitudinal responses at the midpoint, respectively. It is seen that the transient amplitudes are the same in 1-

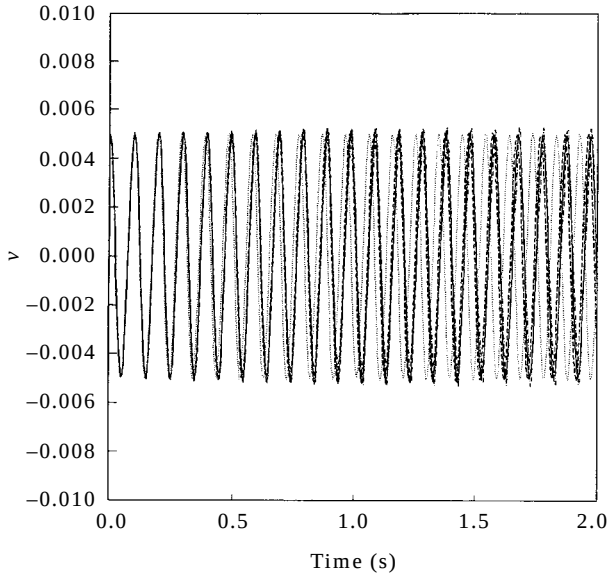

Figure 3. The response of the simply supported cable at midpoint with various element numbers: - · -, $n = 32$; —, $n = 16$; ---, $n = 8$; …, $n = 4$.

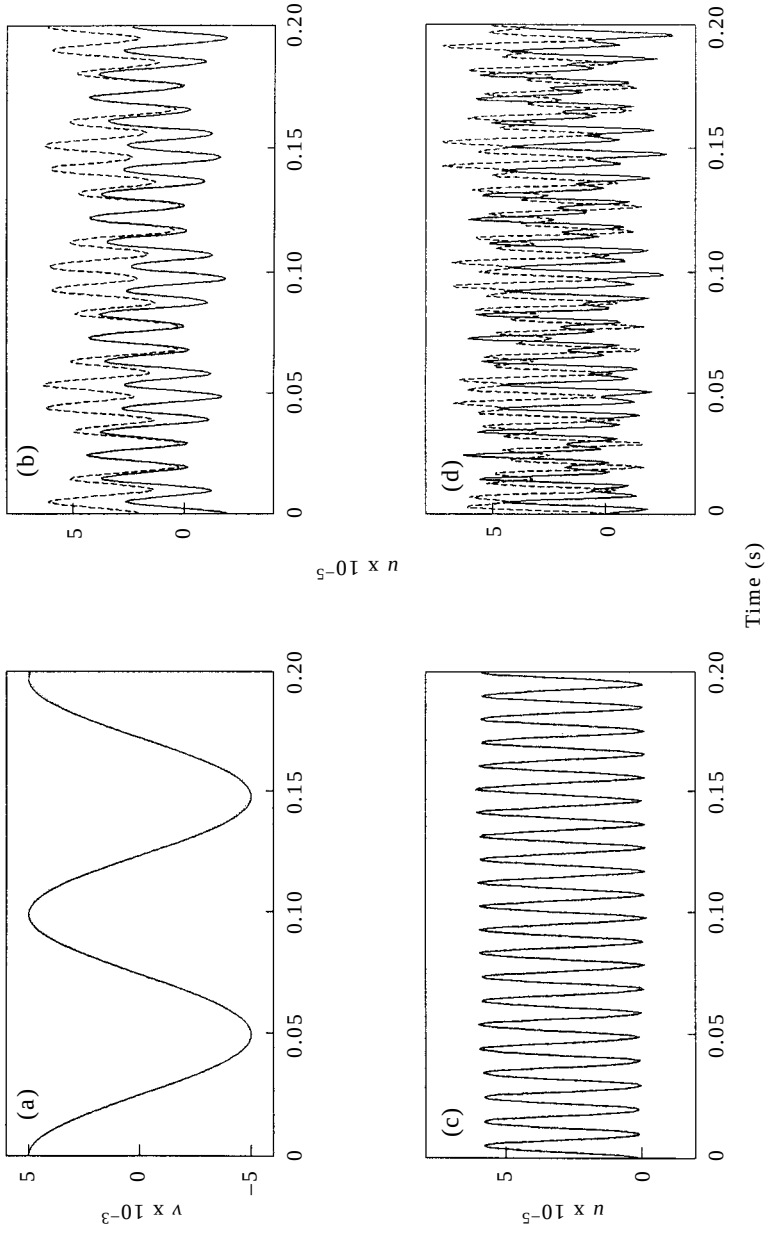

Figure 4. The responses of the cable with constant length $l_0 = 0{\cdot}5$ m, initial displacement $b = 0{\cdot}005$ m, initial condition $v(x, 0) = b \sin(\pi x/l_0)$. In Figures (a) and (c): –, 2-D model with $u(x, 0) = -\pi b^2/8l_0 \sin(2\pi x/l_0)$; ---, 2-D model with $u(x, 0) = 0$; ... 1-D model with (a) $v(\frac{1}{4}l_0, t)$ versus t, (c) $u(\frac{1}{4}l_0, t)$ versus t. In Figures (b) and (d): —, $\frac{1}{4}l_0$; ---, $\frac{3}{4}l_0$. (b) 2-D Model with $u(x, 0) = -\pi b^2/8l_0 \sin(2\pi x/l_0)$; (d) 2-D model with $u(x, 0) = 0$.

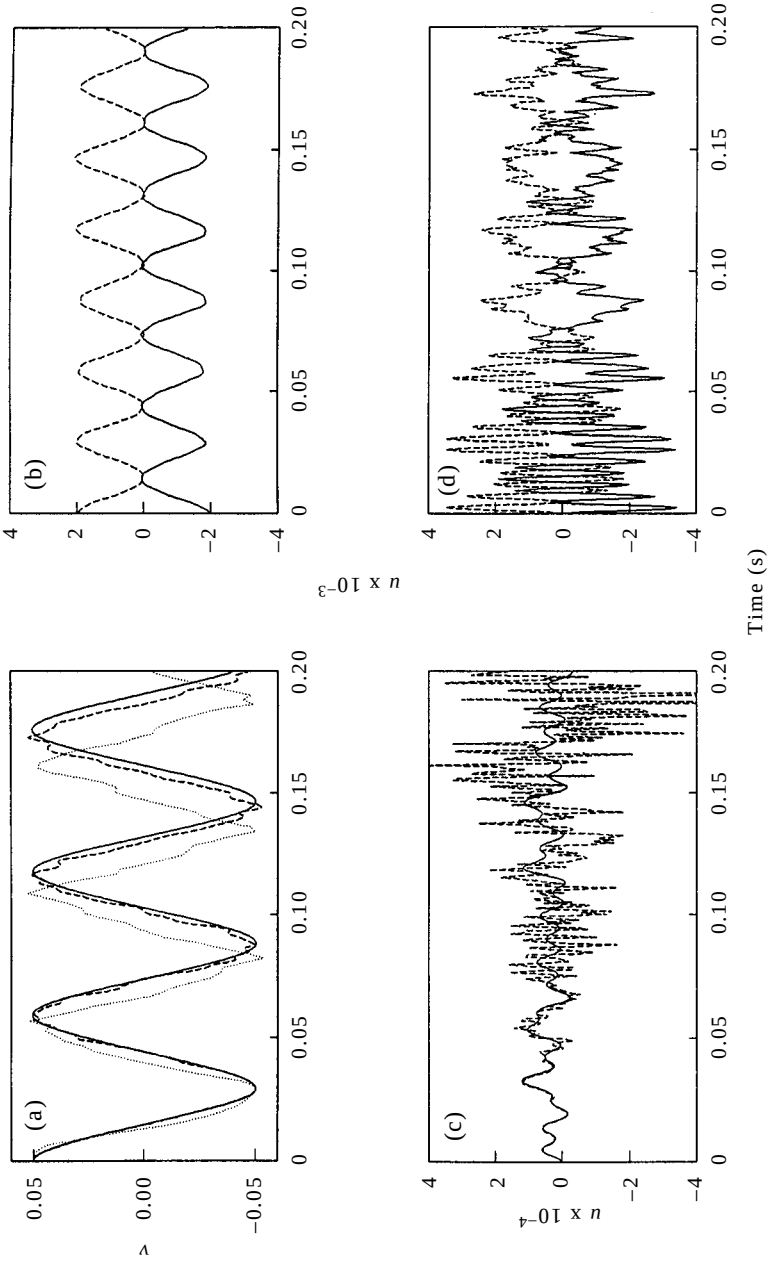

Figure 5. The responses of the cable with constant length $l_0 = 0{\cdot}5$ m, initial displacement $b = 0{\cdot}05$ m, initial condition $v(x, 0) = b \sin(\pi x/l_0)$. In Figures (a) and (c): —, 2-D model with $u(x, 0) = -\pi b^2/8l_0 \sin(2\pi x/l_0)$; ---, 2-D model with $u(x, 0) = 0$; . . . 1-D model with (a) $v(l/2, t)$ versus t, (c) $u(l/2, t)$ versus t. In Figures (b) and (d): —, $\frac{1}{4}l_0$; ---, $\frac{3}{4}l_0$. (b) 2-D Model with $u(x, 0) = -\pi b^2/8l_0 \sin(2\pi x/l_0)$; (d) 2-D model with $u(x, 0) = 0$.

and 2-D models as the initial displacement $b = 0{\cdot}005$ m is given. The frequencies in both the transverse and longitudinal directions agree with the theoretical values. Figures 4(b) and (d) show the longitudinal displacements at $\frac{1}{4}l_0$ and $\frac{3}{4}l_0$. The initial conditions given in equation (35) apply to Figure 4(b), while in Figure 4(d), $u(x, 0) = 0$. It is seen that the longitudinal amplitudes shown in Figure 4(b) are smoother and there is less high-frequency interaction than in Figure 4(d).

Figures 5(a) and (c) show respectively the transient transverse and longitudinal amplitudes with initial displacement $b = 0{\cdot}05$ m, which is ten times that of Figure 4. It is seen that the transient amplitudes are not the same in 1- and 2-D modes. The frequency obtained by 1-D model analysis is larger than that by 2-D model analysis. The reason is that as the vibrations are constrained in the 1-D model, the stiffness of the cable will increase and the frequency of vibrations also increases. The transient amplitudes shown in Figures 5(b) and (d) have the same phenomenon as in Figures 4(b) and (d).

Figure 6 shows the longitudinal and the transverse responses of the cable with a constant-speed motion in the axial direction. As the cable is deployed as shown in Figures 6(a) and (b), the frequency of oscillation decreases but the amplitudes increase. This behavior is due to the decrease in the cable stiffness as the cable length increases. When the cable is retracted as shown in Figures 6(c) and (d), the frequency of oscillation increases and the transient amplitudes decrease. Moreover, the frequency of the cable with initial tension $H = 100N + \rho g(l - x)N$ is larger than that with constant tension $H = 100N$. The frequency of non-linear vibrations is larger than that of linear vibrations in both deployment and retraction.

4.4. FLEXIBLE PENDULUM SYSTEM

As shown in Figure 2(b), the cable is wound on a drum at the top end and attached to a mass at the bottom end. When the attached mass is larger than the mass of the cable, the system is like a pendulum. In the following numerical examples, all the dimensions and properties of the cable are the same as in the previous examples.

Figures 7(a) and (b) show the longitudinal and transverse amplitudes of such a pendulum system, respectively. The system has an initial transverse displacement $v(x, 0) = bx/l_0$ which is proportional to the cable length and is released from rest. Figure 7(a) shows the longitudinal amplitudes at the free end (solid line) and midpoint (dash line) of the cable. The longitudinal amplitudes at the midpoint of the cable exhibit two frequencies. One is

$$\frac{1}{2\pi}\sqrt{\frac{EA}{lm}} = 7{\cdot}05 \text{ Hz}$$

which is due to the pendulum with spring stiffness $k = EA/l$ and the mass m. The other is a high frequency

$$\frac{1}{2\pi}\sqrt{\frac{EA}{\rho l}}$$

which is the frequency of a tight cable in the axial direction. The transverse amplitudes at the free end (solid line) and midpoint (dash line) of the cable are shown in Figure 7(b).

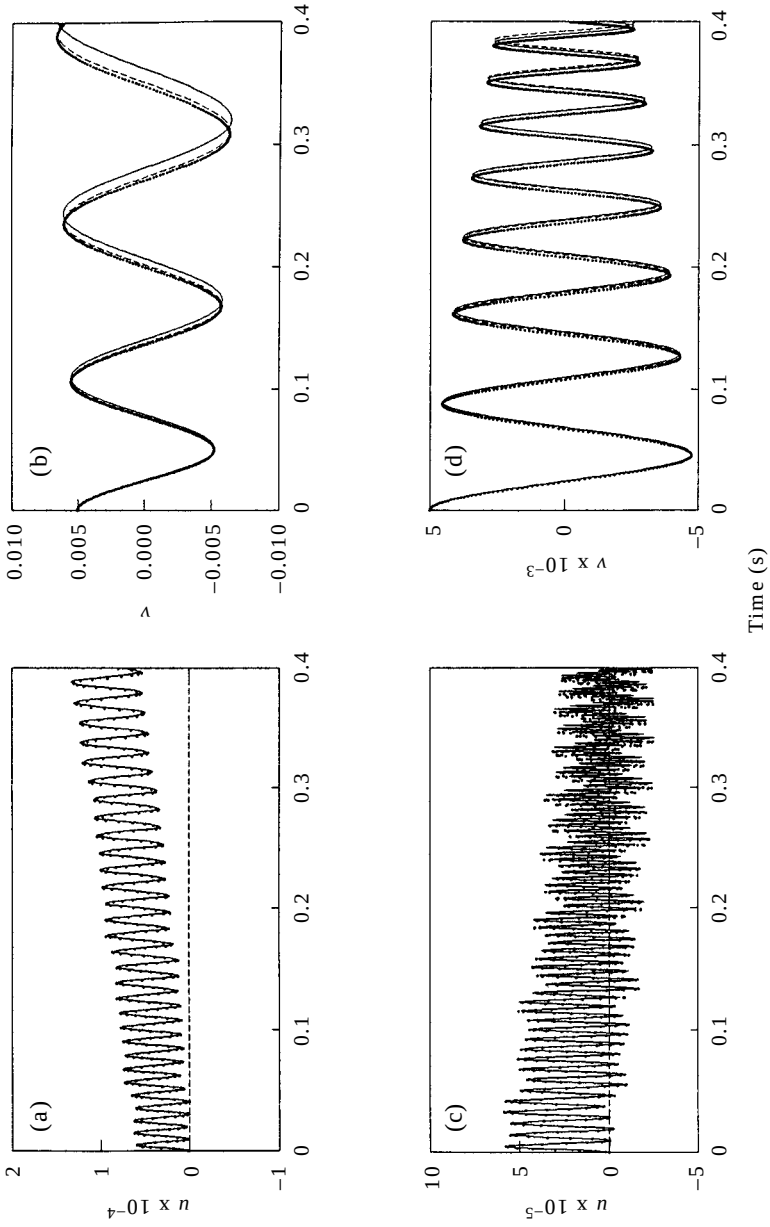

Figure 6. The responses of the cable with the constant-speed axial motion. $l(t) = l_0 + v_0 t$, $l_0 = 0{\cdot}5$ m, $v(x, 0) = b \sin(\pi x/l_0)$, $b = 0{\cdot}01 l_0$. In Figures (a) and (b) $v_0 = 1$ m/s. In Figures (c) and (d) $v_0 = -1$ m/s. (a) Longitudinal displacements $v_0 = 1$ m/s; (b) transverse displacements $v_0 = 1$ m/s; (c) longitudinal displacements $v_0 = -1$ m/s; (d) transverse displacements $v_0 = -1$ m/s. —, Non-linear vibration, $H = 100\ N$; ···, non-linear vibration, $H = 100\ N + \rho g(l - x)N$; ---, linear vibration, $H = 100\ N + \rho g(l - x)N$.

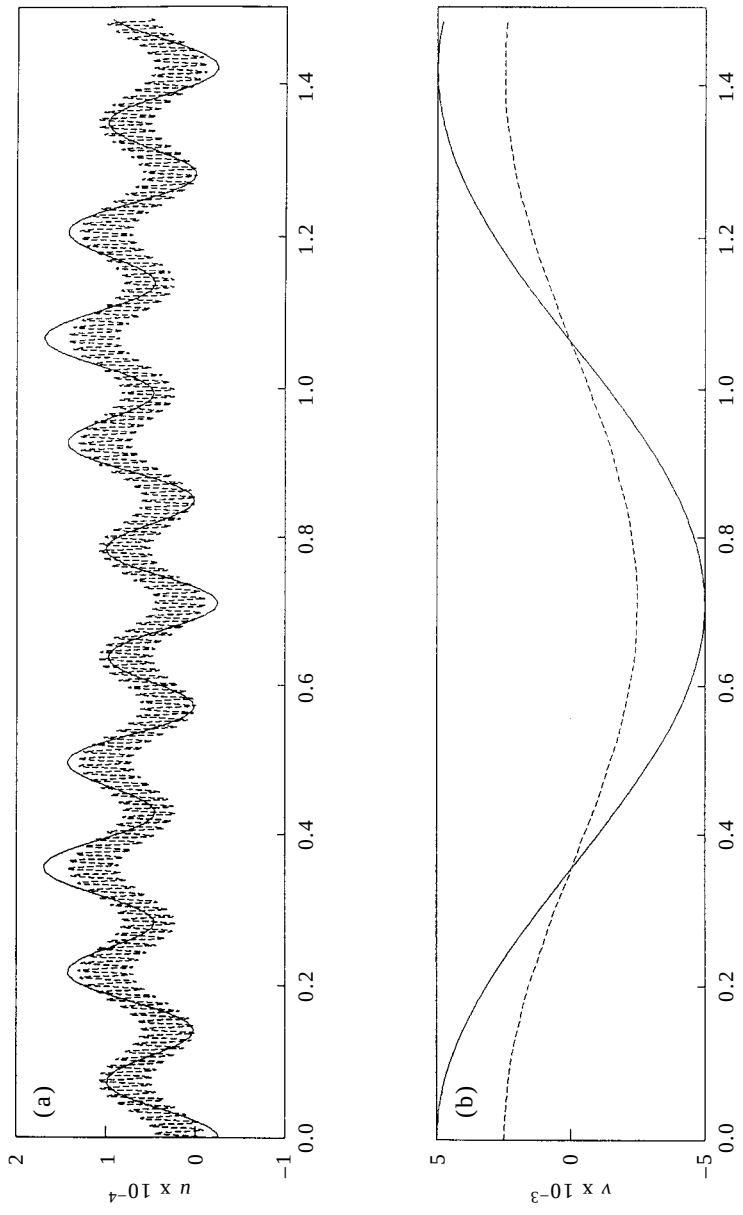

Figure 7. The responses of the cable with fixed-free ends. $l_0 = 0{\cdot}5$ m, $v(x, 0) = bx/l_0$, $b = 0{\cdot}01l_0$. —, Free end of the cable; ---, midpoint of the cable. (a) Longitudinal amplitudes; (b) transverse amplitudes.

The period of the transverse vibration is about 1·4 s. This is close to the theoretic value

$$2\pi\sqrt{\frac{l}{g}} = 1{\cdot}42 \text{ s}$$

of a pendulum with small angle vibrations.

Figures 8(a) and (b) show the longitudinal and transverse amplitudes of the cable, respectively. The cable has two fixed ends and the initial displacement is shown in Figure 2(c). Since the attached mass is larger than that of the cable, the phenomenon of the longitudinal responses [Figure 8(a)] is similar to that in Figure 7(a). The transverse vibrations (dash line) at the midpoint of the cable shown in Figure 8(b), are similar to those in Figure 4(a). However, the transverse amplitudes (solid line) at the free end are almost zero.

Figure 9 shows the longitudinal and transverse amplitudes of the model shown in Figure 2(b) with a time-varying length. The initial length and the initial conditions are the same as in Figure 7. It is seen that as the cable length increases—shown in Figures 9(a) and (c)—the frequency of oscillation decreases but the amplitudes increase. When the cable length decreases—shown in Figures 9(b) and (d)—the frequency of oscillation increases and the amplitudes decrease. The phenomenon is similar to that shown in Figure 6.

4.5. UNDERWATER VIBRATION

Figure 10 shows the non-linear transient amplitudes of the midpoint of the underwater cable using a 3-D model. Initial displacements in the x and y directions are given in equations (35) and (34), respectively. The solid lines denote the amplitudes of the cable under the fluid velocity 0·5 m/s in the z direction and the dash lines denote those with zero fluid velocity. Figures 10(a)–(c) correspond to the transient amplitudes in the x, y and z directions, respectively. In Figure 10(a), the initial axial amplitude is zero and is excited by the non-linear terms. It is shown in Figure 10(b) that the hydrodynamic force decreases the transient amplitudes in the y direction. However, the amplitudes in the z direction are increases by the hydrodynamic force as shown in Figure 10(c).

Figure 11 shows the transient amplitudes of an underwater cable by using a 2-D model. All parameters and initial conditions are the same as those in Figure 6. Because of the action of the hydrodynamic force, both the longitudinal amplitudes shown in Figure 11(a) and the transverse amplitudes shown in Figure 11(b) decrease regardless of whether there is a decrease or an increase in the cable length. Figure 12 shows the transient amplitudes of a time-dependent cable. A 2-D model is used in the analysis and the fluid velocity is $v_f = 0{\cdot}5$ m/s in the y direction. It is seen that the longitudinal amplitudes shown in Figure 12(a) decrease for both deployment and retraction, and the transverse amplitudes shown in Figure 12(b) increase rapidly for deployment and decrease for retraction.

Figure 13 shows the transverse amplitudes with the sinusoidal axial motion which is expressed in equation (31). The steady state velocity is $v_0 = 0$, and the amplitude and frequency of the perturbing velocity are $v_1 = 0{\cdot}5$ m/s and $\omega = 2\Omega$, respectively, where Ω is the first natural frequency of the cable in the transverse vibrations. A 1-D model is used in the analysis. The transient amplitudes of linear analysis, non-linear analysis and underwater vibrations are shown and it can be seen that the parametric resonance occurs for the linear analysis, and the amplitudes diverge. The beating phenomenon occurs for the non-linear system and the amplitudes decrease for the underwater cable.

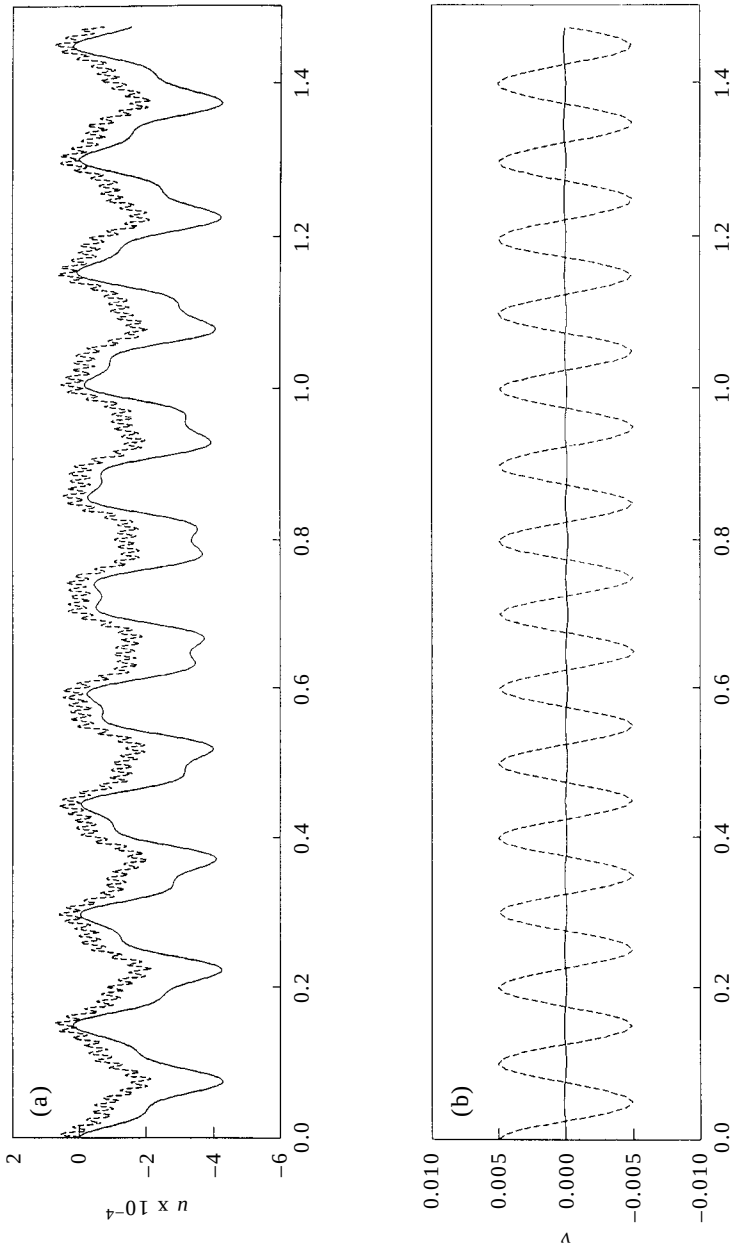

Figure 8. The responses of the cable with fixed-free ends. $l_0 = 0{\cdot}5$ m, $v(x, 0) = b \sin(\pi x/l_0)$, $b = 0{\cdot}01 l_0$. —, Free end of the cable; ---, midpoint of the cable. (a) Longitudinal amplitudes; (b) transverse amplitudes.

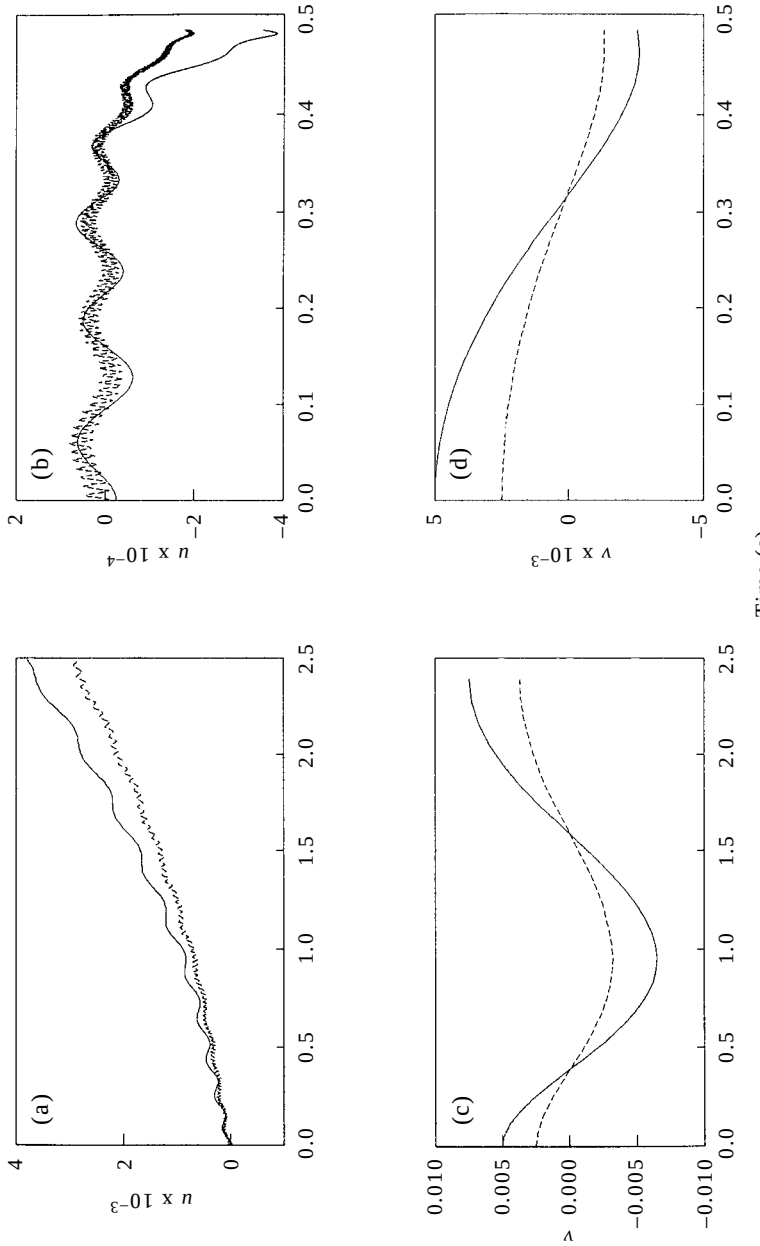

Figure 9. The responses of the time-dependent cable with fixed-free ends. Initial length $l_0 = 0{\cdot}5$ m, initial displacement $v(x, 0) = bx/l_0$, $b = 0{\cdot}01l_0$. —, Free end of the cable; ---, midpoint of the cable. (a) Longitudinal amplitudes with $\dot{x} = 1\ m/s$; (b) longitudinal amplitudes with $\dot{x} = -1\ m/s$; (c) transverse amplitudes with $\dot{x} = 1$ m/s; (d) transverse amplitudes with $\dot{x} = -1$ m/s.

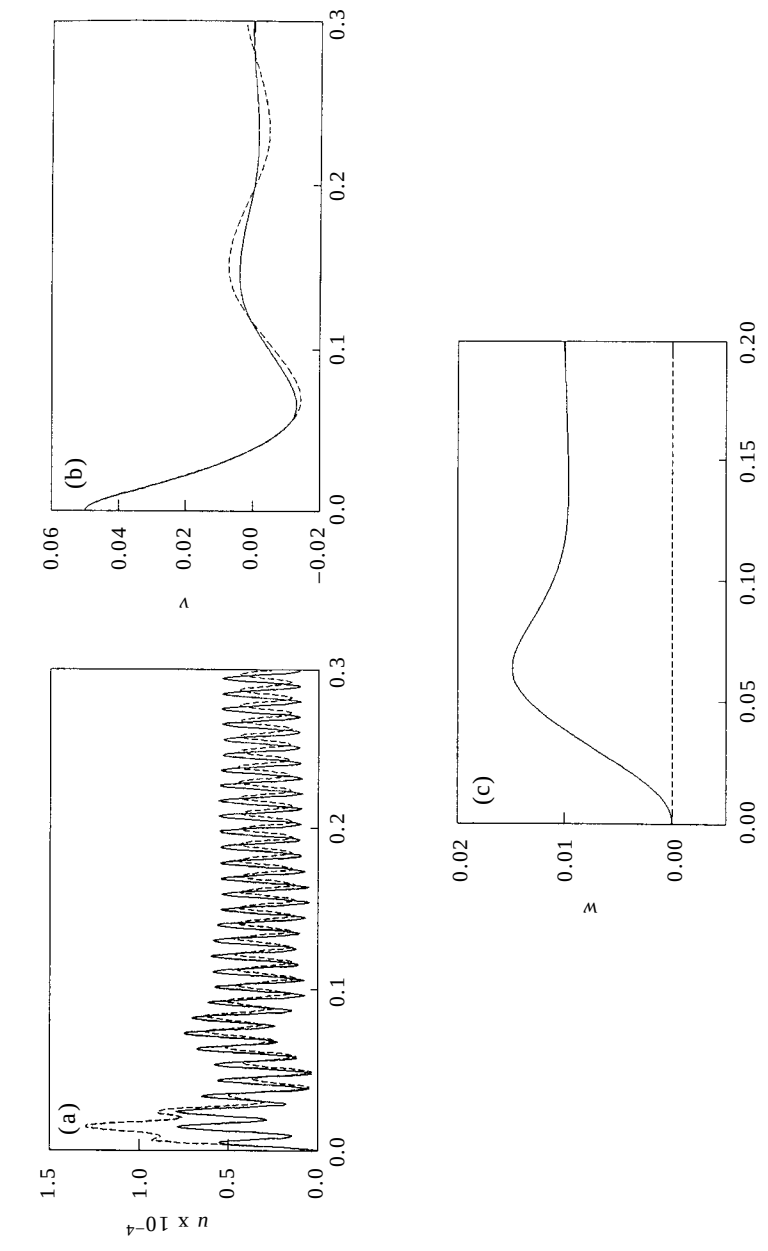

Figure 10. The responses of cable using a 3-D model with length $l_0 = 0{\cdot}5$ m. The initial displacements are $v(x, 0) = b \sin(\pi x/l_0)$, $u(x, 0) = -\pi b^2/8l_0 \sin(2\pi x/l_0)$ and $w(x, 0) = 0$ where $b = 0{\cdot}1l_0$. —, Fluid velocity $\mathbf{v}_f = 0{\cdot}5\mathbf{k}$(m/s); ---, fluid velocity $\mathbf{v}_f = 0$. (a) $u(l/2, t)$ versus t; (b) $v(l/2, t)$ versus t; (c) $w(l/2, t)$ versus t.

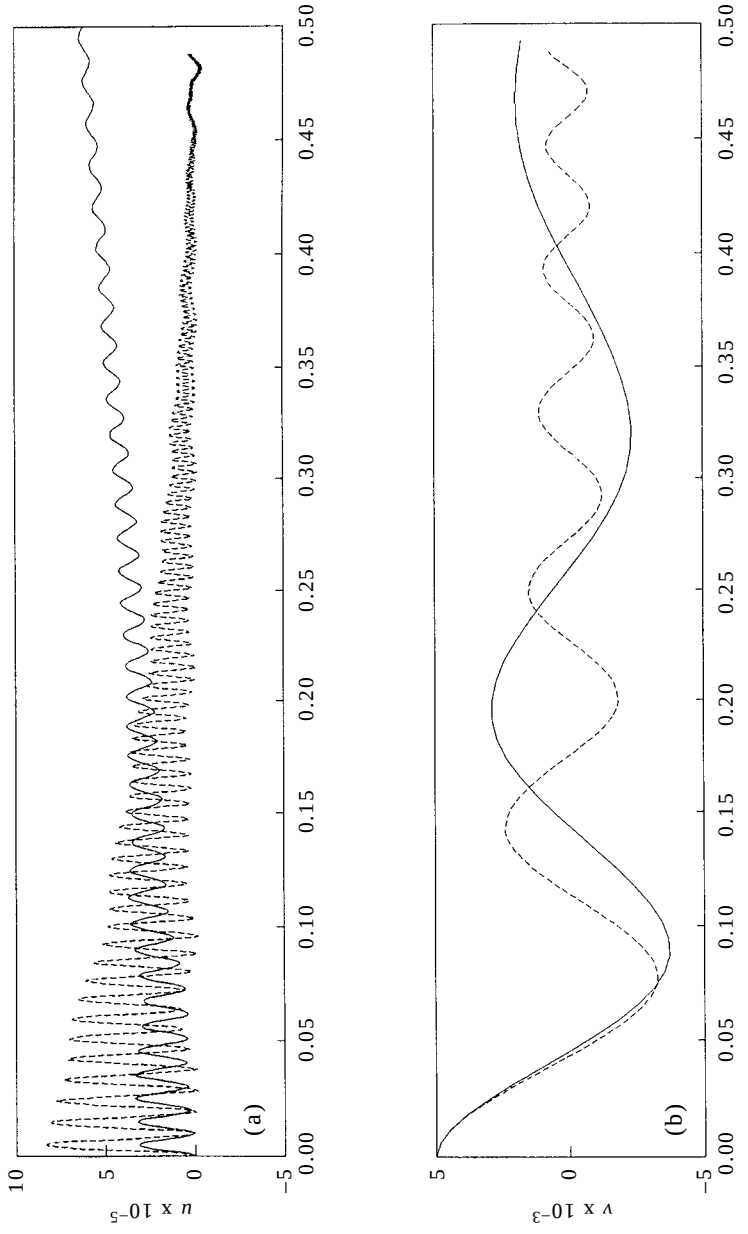

Figure 11. The responses of an underwater cable with time-dependent length, $l(t) = l_0 + v_0 t$, $l_0 = 0{\cdot}5$ m. The intial conditions are $u(x, 0) = 0$, $v(x, 0) = b \sin(\pi x/l_0)$, $b = 0{\cdot}01 l_0$, $v_f = 0$. —, $v_0 = 1$ m/s; ---, $v_0 = -1$ m/s. (a) $u(l/2, t)$ versus t; (b) $v(l/2, t)$ versus t.

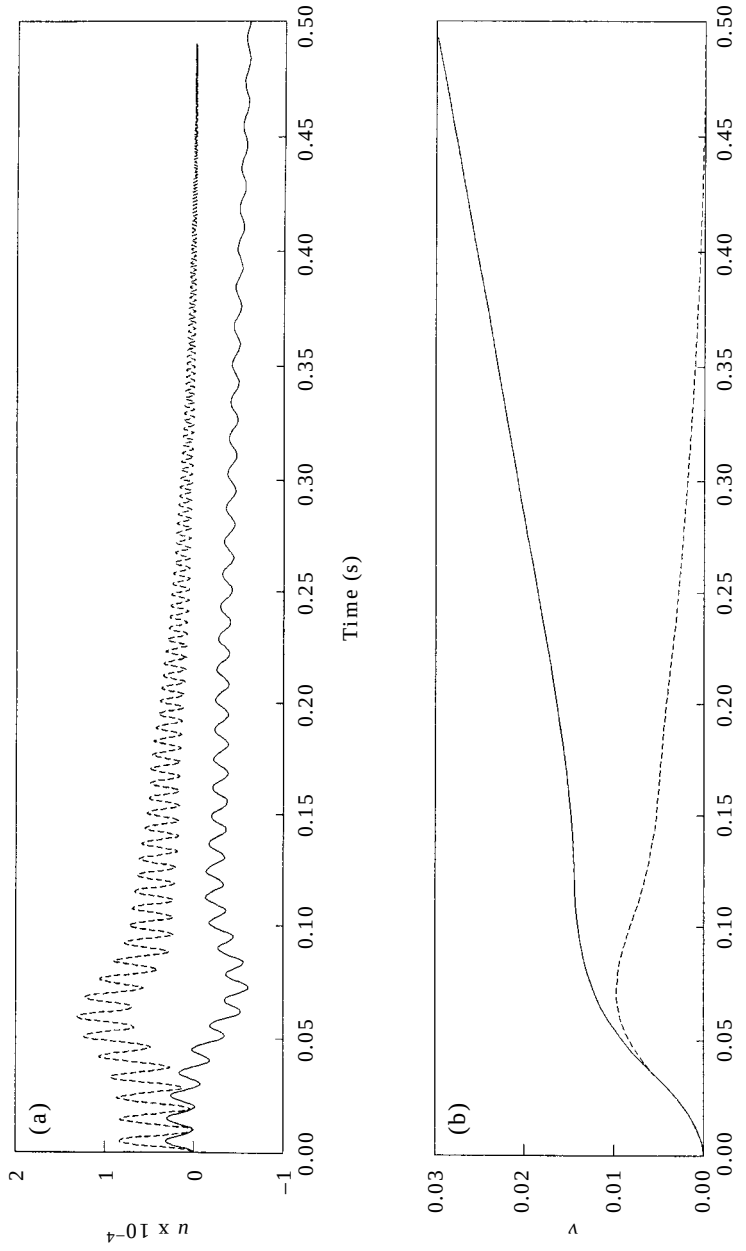

Figure 12. The responses of an underwater cable with the constant-speed axial motion, $l(t) = l_0 + v_0 t$, $l_0 = 0{\cdot}5$ m. The initial conditions are $u(x, 0) = 0$ and $v(x, 0) = 0$. Fluid velocity is $\mathbf{v}_f = 0{\cdot}5\mathbf{j}$(m/s). —, $v_0 = 1$ m/s; ---, $v_0 = -1$ m/s. (a) $u(l/2, t)$ versus t; (b) $v(l/2, t)$ versus t.

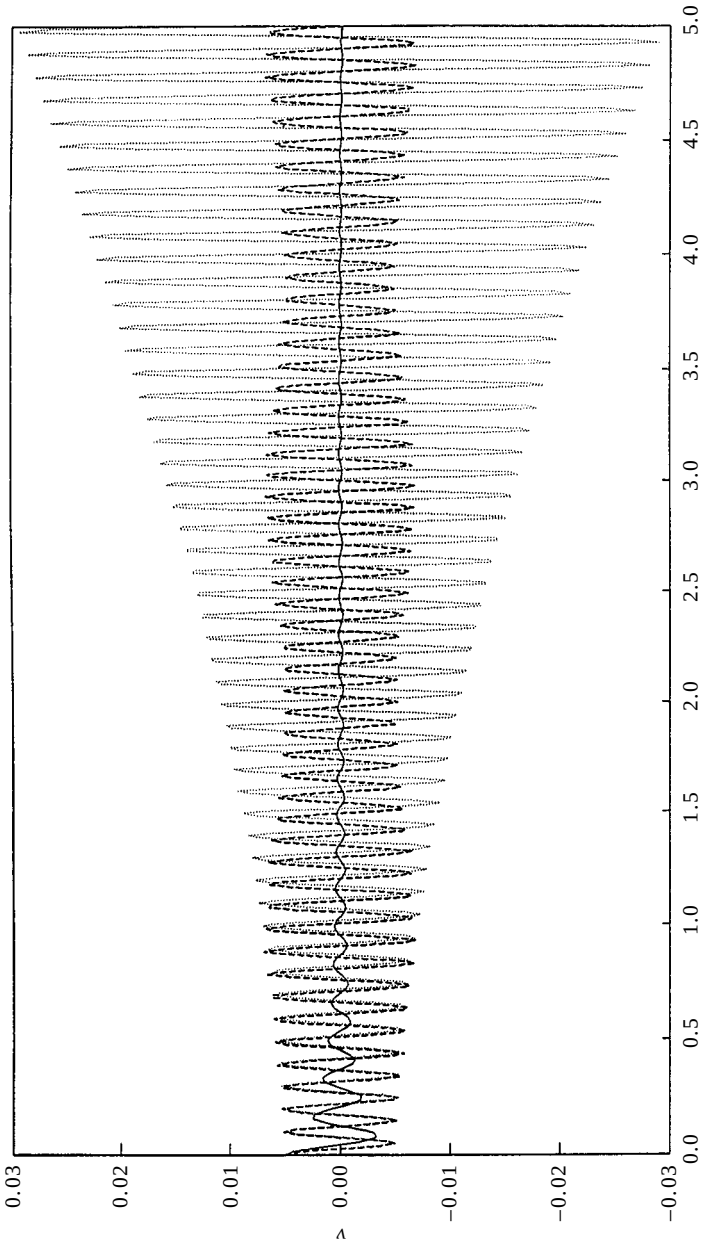

Figure 13. The responses of a simply supported cable with the sinusoidal axial motion, $\dot{x}(t) = 0{\cdot}5 \sin \omega t$, $\omega = 2\Omega$. The initial conditions are, $v(x, 0) = b \sin(\pi x/l_0)$, $b = 0{\cdot}01 l_0$, $l_0 = 0{\cdot}5$ m. —, Underwater vibration; ---, non-linear analysis; ..., linear analysis.

5. CONCLUSION

The finite element method was used to analyze the vibrations of a 3-D cable with time-dependent length. According to the numerical simulations with different axial-motion, boundary conditions and the hydrodynamic forces, the conclusions drawn are: (1) the initial condition has a great influence on the responses of vibration for the non-linear analysis of the cable. It is found that the frequency obtained from a 1-D transverse model analysis is larger than that from a 2-D model (longitudinal and transverse) analysis. (2) As the tension in the cable due to gravity is considered, the frequency is larger than that with constant tension. (3) The effects of fluid on the moving cable are the damping of the vibration amplitudes and the decrease in the frequency of oscillation. (4) As the axial motion is sinusoidal, the parametric resonance occurs for the linear analysis, the beating phenomenon occurs for the non-linear system and the amplitudes decrease for the underwater cable.

ACKNOWLEDGEMENTS

The authors are greatly indebted to the National Science Council of the Republic of China for supporting the research through contract No. NSC 85-2212-E-033-006.

REFERENCES

1. J. V. Sanders 1982 *Ocean Engineering* **9**, 483–499. A three-dimensional dynamic analysis of a towed system.
2. T. N. Delmer, T. C. Stephens and J. M. Coe 1983 *Ocean Engineering* **10**, 119–132. Numerical simulation of towed cable.
3. C. M. Ablow and S. Schechter 1983 *Ocean Engineering* **10**, 443–457. Numerical simulation of undersea cable dynamics.
4. F. Milinazzo and M. Wilkie 1984 *Ocean Engineering* **14**, 513–526. An efficient algorithm for simulating the dynamics of towed cable system.
5. T. N. Delmer, T. C. Stephens and J. A. Tremills 1988 *Ocean Engineering* **15**, 511–548. Numerical simulation of cable-towed acoustic arrays.
6. M. Hann 1994 *Transactions of the American Society of Mechanical Engineers*, *Engineering Systems Design and Analysis* **8**, 625–636. Theoretical and experimental investigation procedure of the submersible hoisting systems.
7. F. S. Hover, M. A. Grosenbaugh and M. S. Triantafyllou 1994 *IEEE Journal of Oceanic Engineering* **19**, 449–457. Calculation of dynamic motions and tensions in towed underwater cables.
8. A. K. Banerjee and V. N. Do 1994 *Journal of Guidance*, *Control*, *and Dynamics* **17**, 1327–1332. Deployment control of a cable connecting a ship to an underwater vehicle.
9. N. U. Khan and K. A. Ansar 1986 *Computer and Structures* **22**, 311–334. On the dynamics of a multicomponent mooring line.
10. J. A. Wickert and C. D. Mote 1988 *Shock and Vibration Digest* **20**, 3–13. Current research on the vibrations and stability of axially moving materials.
11. B. Tabarrok, C. M. Leech and Y. I. Kim 1974 *Journal of Franklin Institute* **297**, 201–220. On the dynamics of axially moving beams.
12. P. K. C. Wang and J.-D. Wei 1987 *Journal of Sound and Vibration* **116**, 149–160. Vibrations in a moving flexible robot arm.
13. J. Yuh and T. Young 1991 *Transactions of the American Society of Mechanical Engineers*, *Journal of Dynamic Systems*, *Measurement*, *and Control* **113**, 34–40. Dynamic modeling of an axially moving beam in rotation: simulation and experiment.
14. R. F. Fung and W. H. Cheng 1993 *Journal of the Chinese Society of Mechanical Engineers* **12**, 229–239. Free vibration of a string/slider non-linear coupling system.
15. T. Kotera 1988 *Nippon Kikai Gakkai Ronbunshu*, *C Hen/Transactions of the Japan Society of Mechanical Engineers*, *Part C* **54**, 2597–2604. Vibrations of strings with time-varying length.

16. T. KOTERA and R. KAWAI 1988 *Nippon Kikai Gakkai Ronbunshu*, *C Hen/Transactions of the Japan Society of Mechanical Engineers*, *Part C* **54**, 1–15. Vibrations of string with time-varying length.
17. T. KOTERA and R. KAWAI 1988 *Nippon Kikai Gakkai Ronbunshu*, *C Hen/Transactions of the Japan Society of Mechanical Engineers*, *Part C* **54**, 16–21. Vibrations of string with time-varying length.
18. T. KOTERA and R. KAWAI 1988 *Transactions of the Japan Society of Mechanical Engineers*, *International Journal Series III*, *Vibration Control Engineering for Industry* **31**, 524–529. Vibrations of string with time-varying length.
19. T. KOTERA and T. KANAYAMA 1993 *Nippon Kikai Gakkai Ronbunshu*, *C Hen/Transactions of the Japan Society of Mechanical Engineers*, *Part C* **59**, 2421–2424. Vibrations of string with time-varying length.
20. M. STYLIANOU and B. TABARROK 1994 *Journal of Sound and Vibration* **178**, 433–453. Finite element analysis of an axially moving beam, Part I: time integration.
21. B. O. AL-BEDOOR and Y. A. KHULIEF 1996 *Journal of Sound and Vibration* **190**, 195–206. Vibrational motion of an elastic beam with prismatic and revolute joints.
22. Y. TERUMICHI, M. OHTSUKA, Y. FUKAWA, M. YOSHIZAWA and Y. TSUJIOKA 1993 *Transactions of the American Society of Mechanical Engineers*, *Dynamics and Vibration of Time-Varying Systems and Structures* **56**. Nonstationary vibrations of a string with time-varying length and mass-spring system attached at the lower end.
23. A. LUONGO, G. REGA and F. VESTRONI 1984 *International Journal of Non-Linear Mechanics* **19**, 39–52. Planar non-linear free vibrations of an elastic cable.
24. J. A. WICKERT and C. D. MOTE JR. 1990 *Transactions of the American Society of Mechanical Engineers*, *Journal of Applied Mechanics* **57**, 738–744. Classical vibration analysis of axially moving continua.
25. R. L. WEBSTER 1976 *General Electric Technical Information Series Report No. R76EMH2*, *Syracuse*, *New York*. An application of the finite element method to the determination of non-linear static and dynamic response of underwater cable structures.
26. A. W. LEISSA and A. M. SAAD 1994 *Transactions of the American Society of Mechanical Engineers*, *Journal of Applied Mechanics* **61**, 296–301. Large-amplitude vibrations of strings.
27. M. J. LEE 1996 *Master Thesis*, *Chung Yuan University*, *Taiwan*, *Republic of China*. Finite element analysis of a three-dimensional underwater cable with time-dependent length.

APPENDIX

For the element kinetic and element strain energies in (23)

$$T_j = \frac{\rho}{2}[\mathbf{q}_{uj}^T\mathbf{k}_{j1}\mathbf{q}_{uj} + 2\mathbf{q}_{uj}^T\mathbf{c}_{j1}\dot{\mathbf{q}}_{uj} + \dot{\mathbf{q}}_{uj}^T\mathbf{m}_j\dot{\mathbf{q}}_{uj} + \dot{x}^2\mathbf{q}_{uj}^T\mathbf{k}_{j3}\mathbf{q}_{uj} + 2\dot{x}\mathbf{q}_{uj}^T\mathbf{k}_{j2}\mathbf{q}_{uj} + 2\dot{x}\dot{\mathbf{q}}_{uj}^T\mathbf{c}_{j2}\mathbf{q}_{uj}]$$

$$+\frac{\rho}{2}[\mathbf{q}_{vj}^T\mathbf{k}_{j1}\mathbf{q}_{vj} + 2\mathbf{q}_{vj}^T\mathbf{c}_{j1}\dot{\mathbf{q}}_{vj} + \dot{\mathbf{q}}_{vj}^T\mathbf{m}_j\dot{\mathbf{q}}_{vj} + \dot{x}^2\mathbf{q}_{vj}^T\mathbf{k}_{j3}\mathbf{q}_{vj} + 2\dot{x}\mathbf{q}_{vj}^T\mathbf{k}_{j2}\mathbf{q}_{vj} + 2\dot{x}\dot{\mathbf{q}}_{vj}^T\mathbf{c}_{j2}\mathbf{q}_{vj}]$$

$$+\frac{\rho}{2}[\mathbf{q}_{wj}^T\mathbf{k}_{j1}\mathbf{q}_{wj} + 2\mathbf{q}_{wj}^T\mathbf{c}_{j1}\dot{\mathbf{q}}_{wj} + \dot{\mathbf{q}}_{wj}^T\mathbf{m}_j\dot{\mathbf{q}}_{wj} + \dot{x}^2\mathbf{q}_{wj}^T\mathbf{k}_{j3}\mathbf{q}_{wj} + 2\dot{x}\mathbf{q}_{wj}^T\mathbf{k}_{j2}\mathbf{q}_{wj} + 2\dot{x}\dot{\mathbf{q}}_{wj}^T\mathbf{c}_{j2}\mathbf{q}_{wj}]$$

$$+\frac{\rho}{2}\int_{x_j}^{x_{j+1}} \dot{x}^2\,\mathrm{d}x + \rho[\dot{x}\mathbf{f}_{j2}\mathbf{q}_{uj} + \dot{x}\mathbf{f}_{j3}\dot{\mathbf{q}}_{uj} + \dot{x}^2\mathbf{f}_{j1}\mathbf{q}_{uj}], \tag{A1}$$

$$U_j = H(1+\epsilon_0)[\mathbf{f}_{j1}\mathbf{q}_{uj} + \tfrac{1}{2}(\mathbf{q}_{uj}^T\mathbf{k}_{j3}\mathbf{q}_{uj} + \mathbf{q}_{vj}^T\mathbf{k}_{j3}\mathbf{q}_{vj} + \mathbf{q}_{wj}^T\mathbf{k}_{j3}\mathbf{q}_{wj})] + \tfrac{1}{2}k(1+\epsilon_0)[\mathbf{q}_{uj}^T\mathbf{k}_{j3}\mathbf{q}_{uj}]$$

$$+\tfrac{1}{2}k(1+\epsilon_0)\int_{x_j}^{x_{j+1}} \{\mathbf{N}_{jx}\mathbf{q}_{uj}(\mathbf{q}_{uj}^T\mathbf{N}_{jx}^T\mathbf{N}_{jx}\mathbf{q}_{uj} + \mathbf{q}_{vj}^T\mathbf{N}_{jx}^T\mathbf{N}_{jx}\mathbf{q}_{vj} + \mathbf{q}_{wj}^T\mathbf{N}_{jx}^T\mathbf{N}_{jx}\mathbf{q}_{wj})$$

$$+\tfrac{1}{4}(\mathbf{q}_{uj}^T\mathbf{N}_{jx}^T\mathbf{N}_{jx}\mathbf{q}_{uj} + \mathbf{q}_{vj}^T\mathbf{N}_{jx}^T\mathbf{N}_{jx}\mathbf{q}_{vj} + \mathbf{q}_{wj}^T\mathbf{N}_{jx}^T\mathbf{N}_{jx}\mathbf{q}_{wj})^2\}\,\mathrm{d}x, \tag{A2}$$

in which $\mathbf{k}_{j1}$, $\mathbf{k}_{j2}$, $\mathbf{k}_{j3}$, $\mathbf{m}_j$, $\mathbf{c}_{j1}$ and $\mathbf{c}_{j2}$ are 2×2 matrices, $\mathbf{f}_{j1}$, $\mathbf{f}_{j2}$ and $\mathbf{f}_{j3}$ are 1×2 matrices. They are defined as

$$\mathbf{k}_{j1} = \int_{x_j}^{x_{j+1}} \mathbf{N}_{jt}^T \mathbf{N}_{jt}\, \mathrm{d}x, \qquad \mathbf{m}_j = \int_{x_j}^{x_{j+1}} \mathbf{N}_j^T \mathbf{N}_j\, \mathrm{d}x,$$

$$\mathbf{k}_{j2} = \int_{x_j}^{x_{j+1}} \mathbf{N}_{jt}^T \mathbf{N}_{jx}\, \mathrm{d}x, \qquad \mathbf{f}_{j1} = \int_{x_j}^{x_{j+1}} \mathbf{N}_{jx}\, \mathrm{d}x,$$

$$\mathbf{k}_{j3} = \int_{x_j}^{x_{j+1}} \mathbf{N}_{jx}^T \mathbf{N}_{jx}\, \mathrm{d}x, \qquad \mathbf{f}_{j2} = \int_{x_j}^{x_{j+1}} \mathbf{N}_{jt}\, \mathrm{d}x,$$

$$\mathbf{c}_{j1} = \int_{x_j}^{x_{j+1}} \mathbf{N}_{jt}^T \mathbf{N}_j\, \mathrm{d}x, \qquad \mathbf{f}_{j3} = \int_{x_j}^{x_{j+1}} \mathbf{N}_j\, \mathrm{d}x,$$

$$\mathbf{c}_{j2} = \int_{x_j}^{x_{j+1}} \mathbf{N}_j^T \mathbf{N}_{jx}\, \mathrm{d}x. \tag{A3}$$

It should be noted that $\mathbf{m}_j$, $\mathbf{k}_{j1}$, $\mathbf{k}_{j2}$ and $\mathbf{k}_{j3}$ are symmetric matrices, $\mathbf{c}_{j1}$ and $\mathbf{c}_{j2}$ are antisymmetric matrices.

The tangent drag force can be expressed as

$$\mathbf{f}_{DT} = |\mathbf{f}_{DT}|\mathbf{t} = |\mathbf{f}_{DT}|t_x\mathbf{i} + |\mathbf{f}_{DT}|t_y\mathbf{j} + |\mathbf{f}_{DT}|t_z\mathbf{k}, \tag{A4}$$

where

$$|\mathbf{f}_{DT}| = C_T\rho_f(d/2)\int_{x_j}^{x_{j+1}} \mathbf{N}_j^T[v_x^2t_x^2 + v_y^2t_y^2 + v_z^2t_z^2 + 2(v_xv_yt_xt_y + v_xv_zt_xt_z + v_yv_zt_yt_z)]\, \mathrm{d}x, \tag{A5}$$

$$\begin{aligned} t_x &= (1 + \mathbf{N}_{jx}\mathbf{q}_{uj})(1 + 2\mathbf{N}_{jx}\mathbf{q}_{uj} + \mathbf{q}_{uj}\mathbf{N}_{jx}\mathbf{N}_{jx}\mathbf{q}_{uj} + \mathbf{q}_{uj}\mathbf{N}_{jx}\mathbf{N}_{jx}\mathbf{q}_{uj} + \mathbf{q}_{uj}\mathbf{N}_{jx}\mathbf{N}_{jx}\mathbf{q}_{uj})^{\frac{1}{2}},\\ t_y &= (1 + \mathbf{N}_{jx}\mathbf{q}_{vj})(1 + 2\mathbf{N}_{jx}\mathbf{q}_{uj} + \mathbf{q}_{uj}\mathbf{N}_{jx}\mathbf{N}_{jx}\mathbf{q}_{uj} + \mathbf{q}_{uj}\mathbf{N}_{jx}\mathbf{N}_{jx}\mathbf{q}_{uj} + \mathbf{q}_{uj}\mathbf{N}_{jx}\mathbf{N}_{jx}\mathbf{q}_{uj})^{\frac{1}{2}},\\ t_z &= (1 + \mathbf{N}_{jx}\mathbf{q}_{wj})(1 + 2\mathbf{N}_{jx}\mathbf{q}_{uj} + \mathbf{q}_{uj}\mathbf{N}_{jx}\mathbf{N}_{jx}\mathbf{q}_{uj} + \mathbf{q}_{uj}\mathbf{N}_{jx}\mathbf{N}_{jx}\mathbf{q}_{uj} + \mathbf{q}_{uj}\mathbf{N}_{jx}\mathbf{N}_{jx}\mathbf{q}_{uj})^{\frac{1}{2}}. \end{aligned} \tag{A6}$$

The normal drag force can be expressed as

$$\mathbf{f}_{DN} = |\mathbf{f}_{DN}|\mathbf{n} = |\mathbf{f}_{DN}|n_x\mathbf{i} + |\mathbf{f}_{DN}|n_y\mathbf{j} + |\mathbf{f}_{DN}|n_z\mathbf{k}, \tag{A7}$$

where

$$\begin{aligned} |\mathbf{f}_{DN}| = C_T\rho_f(d/2)\int_{x_j}^{x_{j+1}} &\mathbf{N}_j^T[v_x^2[(1 - t_x^2)^2 + (t_xt_y)^2 + (t_xt_z)^2] + 2v_xv_y[t_xt_y(t_x^2 + t_y^2 + t_z^2 - 2)]\\ &+ v_y^2[(t_xt_y)^2 + (1 - t_y^2)^2 + (t_yt_z)^2] + 2v_xv_z[t_xt_z(t_x^2 + t_y^2 + t_z^2 - 2)]\\ &+ v_z^2[(t_xt_z)^2 + (t_yt_z)^2 + (1 - t_z^2)^2] + 2v_yv_z[t_yt_z(t_x^2 + t_y^2 + t_z^2 - 2)]\, \mathrm{d}x, \end{aligned} \tag{A8}$$

and **n** is the unit normal vector of the fluid velocity relative to the cable. It can be obtained by

$$\mathbf{n} = \frac{\mathbf{v}_N}{|\mathbf{v}_N|} = (\mathbf{v}_N \cdot \mathbf{v}_N)^{\frac{1}{2}} \cdot \mathbf{v}_N. \tag{A9}$$

The inertia force due to the added mass can be expressed as

$$\begin{aligned}\mathbf{f}_{AM} &= C_M \rho_f A \int_{x_j}^{x_{j+1}} \mathbf{N}_j^T \mathbf{a}_N \, \mathrm{d}x \\ &= C_M \rho_f A \left[\left(\int_{x_j}^{x_{j+1}} \mathbf{N}_j^T a_{Nx} \, \mathrm{d}x \right) \mathbf{i} + \left(\int_{x_j}^{x_{j+1}} \mathbf{N}_j^T a_{Ny} \, \mathrm{d}x \right) \mathbf{j} + \left(\int_{x_j}^{x_{j+1}} \mathbf{N}_j^T a_{Nz} \, \mathrm{d}x \right) \mathbf{k} \right].\end{aligned} \tag{A10}$$

After some manipulations, equation (A10) can be transformed to the following matrix form:

$$\begin{aligned}\mathbf{f}_{AM} = \rho_f A \Bigg(&\begin{bmatrix} \mathbf{M}_{uf} & \mathbf{M}_{uvf} & \mathbf{M}_{uwf} \\ & \mathbf{M}_{vf} & \mathbf{M}_{vwf} \\ sym. & & \mathbf{M}_{wf} \end{bmatrix} \begin{Bmatrix} \mathbf{Q}_u \\ \mathbf{Q}_v \\ \mathbf{Q}_w \end{Bmatrix} + \begin{bmatrix} \mathbf{C}_{uf} & \mathbf{C}_{uvf} & \mathbf{C}_{uwf} \\ & \mathbf{C}_{vf} & \mathbf{C}_{vwf} \\ sym. & & \mathbf{C}_{wf} \end{bmatrix} \begin{Bmatrix} \mathbf{Q}_u \\ \mathbf{Q}_v \\ \mathbf{Q}_w \end{Bmatrix} \\ &+ \begin{bmatrix} \mathbf{K}_{uf} & \mathbf{K}_{uvf} & \mathbf{K}_{uwf} \\ & \mathbf{K}_{vf} & \mathbf{K}_{vwf} \\ sym. & & \mathbf{K}_{wf} \end{bmatrix} \begin{Bmatrix} \mathbf{Q}_u \\ \mathbf{Q}_v \\ \mathbf{Q}_w \end{Bmatrix} + \begin{Bmatrix} \mathbf{F}_{ANu} \\ \mathbf{F}_{ANv} \\ \mathbf{F}_{ANw} \end{Bmatrix} \Bigg).\end{aligned} \tag{A11}$$

All the expressions of the matrices are non-linear and can be found in Lee [27].

For the global equations (29):

$$\begin{gathered}\mathbf{M} = \sum_{j=1}^{n} \mathbf{m}_j, \qquad \mathbf{C} = \sum_{j=1}^{n} \mathbf{c}_j, \qquad \mathbf{K}_u = \sum_{j=1}^{n} \mathbf{k}_{uj}, \qquad \mathbf{K}_v = \mathbf{K}_w = \sum_{j=1}^{n} \mathbf{K}_{vj}, \\ \mathbf{F}_u = \sum_{j=1}^{n} (\mathbf{f}_{uj} - \mathbf{s}_{uj}^0), \qquad \mathbf{F}_v = \sum_{j=1}^{n} \mathbf{f}_{vj}, \qquad \mathbf{F}_w = \sum_{j=1}^{n} \mathbf{f}_{wj}, \\ \mathbf{S}_u = \sum_{j=1}^{n} \mathbf{s}_{uj}, \qquad \mathbf{S}_v = \sum_{j=1}^{n} \mathbf{s}_{vj}, \qquad \mathbf{S}_w = \sum_{j=1}^{n} \mathbf{s}_{wj}, \\ \mathbf{Q}_u = \sum_{j=1}^{n} \mathbf{q}_{uj}, \qquad \mathbf{Q}_v = \sum_{j=1}^{n} \mathbf{q}_{vj}, \qquad \mathbf{Q}_w = \sum_{j=1}^{n} \mathbf{q}_{wj}.\end{gathered} \tag{A12}$$

$$\begin{gathered}\mathbf{m}_{uj} = \mathbf{m}_{vj} = \mathbf{m}_{wj} = \rho \mathbf{m}_j, \\ \mathbf{c}_{uj} = \mathbf{c}_{vj} = \mathbf{c}_{wj} = \rho(2\mathbf{c}_{j1}^T + \dot{x}\mathbf{c}_{j2} - \dot{x}\mathbf{c}_{j2}^T), \\ \mathbf{k}_{uj} = \rho(\ddot{x}\mathbf{c}_{j2} - \dot{x}\mathbf{k}_{j2} - \dot{x}^2\mathbf{k}_{j3} + \mathbf{k}_{j4}^T + \dot{x}\mathbf{k}_{j5}) + (H + k)\mathbf{k}_{j3}, \\ \mathbf{k}_{vj} = \mathbf{k}_{wj} = \rho(\ddot{x}\mathbf{c}_{j2} - \dot{x}\mathbf{k}_{j2} - \dot{x}^2\mathbf{k}_{j3} + \mathbf{k}_{j4}^T + \dot{x}\mathbf{k}_{j5}) + H\mathbf{k}_{j3},\end{gathered}$$

$$\mathbf{k}_{j4} = \int_{x_j}^{x_{j+1}} \mathbf{N}_{jtt}^T \mathbf{N}_j \, \mathrm{d}x, \qquad \mathbf{k}_{j5} = \int_{x_j}^{x_{j+1}} \mathbf{N}_j^T \mathbf{N}_{jxt} \, \mathrm{d}x,$$

$$\mathbf{s}_{uj}^0 = H\mathbf{f}_{j1}^T + \rho(\ddot{x}\mathbf{f}_{j3}^T - g\mathbf{f}_{j3}^T - \dot{x}^2\mathbf{f}_{j1}^T), \qquad \mathbf{s}_{vj}^0 = \mathbf{s}_{wj}^0 = 0, \tag{A13}$$

and the non-linear terms can be rewritten as

$$\begin{aligned} \mathbf{s}_{uj}^n &= \tfrac{1}{2}kS\mathbf{f}_{j1}^T + (\mathbf{N}_{jx}\mathbf{q}_{uj} + \tfrac{1}{2}S)k\mathbf{K}_{j3}\mathbf{q}_{uj}, \\ \mathbf{s}_{vj}^n &= (\mathbf{N}_{jx}\mathbf{q}_{uj} + \tfrac{1}{2}S)k\mathbf{k}_{j3}\mathbf{q}_{vj}, \\ \mathbf{s}_{wj}^n &= (\mathbf{N}_{jx}\mathbf{q}_{uj} + \tfrac{1}{2}S)k\mathbf{k}_{j3}\mathbf{q}_{wj}, \end{aligned} \tag{A14}$$

where

$$S = \mathbf{q}_{uj}^T\mathbf{N}_{jx}^T\mathbf{N}_{jx}\mathbf{q}_{uj} + \mathbf{q}_{vj}^T\mathbf{N}_{jx}^T\mathbf{N}_{jx}\mathbf{q}_{vj} + \mathbf{q}_{wj}^T\mathbf{N}_{jx}^T\mathbf{N}_{jx}\mathbf{q}_{wj}. \tag{A15}$$